Preadsorption Effect of Carbon Monoxide on Reactivity of Cobalt Cluster Cations toward Hydrogen

Arakawa, Masashi
Department of Chemistry, Faculty of Science, Kyushu University

Okada, Daichi
Department of Chemistry, Faculty of Science, Kyushu University

Kono, Satoshi
Department of Chemistry, Faculty of Science, Kyushu University

Terasaki, Akira
Department of Chemistry, Faculty of Science, Kyushu University

出版情報：The Journal of Physical Chemistry A. 124 (47), pp.9751-9756, 2020-11-13. American Chemical Society (ACS)
バージョン：

Preadsorption Effect of Carbon Monoxide on Reactivity of Cobalt Cluster Cations toward Hydrogen

Masashi Arakawa,* *Daichi Okada, Satoshi Kono*, *and Akira Terasaki**

Department of Chemistry, Faculty of Science, Kyushu University, 744 Motooka, Nishi-ku, Fukuoka 819-0395, Japan

ABSTRACT

We report gas-phase reactions of free $Co_n(CO)_m^+$ (n = 3–11, m = 0–2) with H_2, expecting catalytic reaction of coadsorbed CO and H_2 on Co_n^+. Pre-adsorption of CO molecules is found to encourage H_2 adsorption, in particular, on $Co_n(CO)^+$ (n = 5, 8–10). DFT calculations reveal that the reactivity is governed by the molecular-orbital energy of Co_n^+, which is tuned by pre-adsorbed CO molecules. Collision-induced-dissociation experiments performed on $Co_nCOH_2^+$ (n = 8–10) imply that at least a part of the CO and H_2 molecules are bound together on Co_n^+.

1. INTRODUCTION

Gas-phase metal clusters have been attracting much attention as ideal model systems of heterogeneous catalysts because they provide molecular-level insights into metal-mediated catalytic reactions.[1] As well as a model system, a gas-phase cluster itself is of great importance in catalysis, e.g., in chemistry in space. It is a prevalent hypothesis that silicate particles such as pyroxene ($Mg_xFe_{1-x}SiO_3$) and olivine ($Mg_{2x}Fe_{2(1-x)}SiO_4$) work as catalysts to form organic molecules from CO, H_2, and other interstellar gases in the early stage of planetary formation, i.e., in protoplanetary disks.[2] In this context, we recently reported silica ($Si_nO_m^-$) and silicate ($Mg_lSiO_m^-$) cluster anions reacting with CO and H_2O molecules.[3,4] It was found that one of the dangling oxygen atoms present in $Si_nO_m^-$ with compositions of $m \geq 2n + 1$ provides an adsorption site for a CO molecule.[3] The CO adsorption is the first step of formation of organic molecules on free gas-phase clusters, which would be followed by coadsorption and subsequent reaction with another molecule such as H_2.

Here we focus on cobalt clusters; cobalt is known as a catalyst of Fischer–Tropsch reaction, where a mixture of CO and H_2 is converted into long-chain hydrocarbons. It has been demonstrated that such a reaction is catalyzed by cobalt clusters deposited on metal-oxide or carbon-based supports.[5] As for gas-phase free clusters, Fischer–Tropsch reaction is yet to be examined. A related study has been reported on reaction of cobalt cluster cations, Co_n^+, with H_2,[6–8] and with CO.[9] In the reaction of Co_n^+ with H_2, size-dependent reactivity was explained by a frontier orbital model,[7] showing that interaction between the lowest unoccupied molecular orbital (LUMO) of H_2 and the highest occupied molecular orbital (HOMO) of the cluster is essential.

In addition to chemical reaction, infrared spectra of CO adsorbed on gas-phase cobalt clusters have been measured.[10] Size-dependent shifts in the C–O stretching frequency were

explained in terms of back donation of electron density from the metal to the CO π* orbital, which weakens the C–O bond.[10] An effect of H_2 coadsorption on the C–O bond was further examined by infrared spectroscopy,[11] which suggests that coadsorbed H_2 reduces the back donation, i.e., a low H_2 coverage is favored for CO activation. It is thus anticipated that coadsorption of H_2 might change the catalytic property of cobalt clusters. In relation to the coadsorption effect, introduction of H to Co_n^+ enhances the reactivity of Co_n^+ toward NO, which was explained by stabilization of reaction intermediates and products.[12] It is also known that preadsorption of H_2O could enhance the reactivity of a cluster toward CO and O_2 as demonstrated for the gold dimer cation.[13] The enhancement toward CO is reported to be due to weakening of the Au−Au bond upon adsorption of a H_2O molecule, while that toward O_2 is ascribed to electron transfer from H_2O to the cluster.

In the present study, we investigate an effect of CO preadsorption on the reactivity of Co_n^+ toward a H_2 molecule. Collision-induced-dissociation (CID) experiments were performed further to gain insights into the reaction product formed on Co_n^+ upon coadsorption of CO and H_2 molecules.

2. METHODS

2.1. Reaction experiment. The experimental setup has been described in detail elsewhere.[14,15] Briefly, Co_n^+ (n = 3–11) were generated by a magnetron-sputter cluster-ion source, where sputtering of a cobalt plate (Kojundo Chemical Laboratory Co., Ltd., 99.99%) was followed by aggregation of sputtered atoms and ions through collisions with a buffer helium gas (99.99995%) cooled by liquid nitrogen. A pick-up cell was placed downstream of the cluster ion source to produce $Co_n(CO)_m^+$ (m = 0–2), where a CO gas (99.95%) cooled down to about 100 K was introduced continuously to preadsorb CO molecules. The produced cations were mass

selected by a quadrupole mass filter (MAX-4000, Extrel CMS, LLC), guided by radio-frequency (rf) octopole ion guides and quadrupole deflectors, and introduced into a reaction cell consisting of a 40-cm-long linear rf quadrupole ion guide biased by 7 V DC. A continuous flow of a H_2 gas (99.99999%) was introduced into the reaction cell at 298 K. The reactant cations passed through the reaction cell within 200 μs. Product ions were identified by a second quadrupole mass analyzer (MAX-4000, Extrel CMS, LLC) employing a channel electron multiplier (Channeltron 4720, Burle Electro-Optics, Inc.) for an ion detector.

The pressure of H_2 in the reaction cell, P_{H2}, was adjusted to the range between 3–4 × 10^{-1} Pa; the pressure was monitored outside the reaction cell by a residual gas analyzer (RGA100, Stanford Research Systems, Inc.), which was converted to the pressure inside the reaction cell in the same way as reported previously[16] by referring to a reaction cross section of Cr_2^+ with O_2.[17] The collision rate estimated from the gas pressure is about 1 × 10^5 s^{-1}, where the collisional cross section, σ, is evaluated by the Langevin−Gioumousis−Stevenson model,[18]

$$\sigma = \pi e\{(2\alpha/(4\pi\varepsilon_0)^2 E)\}^{1/2}. \qquad (1)$$

Here, α is the polarizability of H_2 (0.81 $Å^3$), e the elementary charge, ε_0 the vacuum dielectric constant, k Boltzmann's constant, T the temperature, and E the collision energy in the center-of-mass frame. The collision energy of the clusters with H_2 was 7 eV in the laboratory frame, which corresponds to 0.08 through 0.02 eV in the center-of-mass frame for Co_3^+ through $Co_{11}(CO)_2^+$, respectively.

2.2. Collision-induced-dissociation experiment. Collision-induced-dissociation (CID) experiment was performed on $Co_nCOH_2^+$ (n = 8–10) by the experimental setup described above. Bare Co_n^+ clusters passed through the pick-up cell filled with a mixture of CO and H_2 gases, which was cooled down to about 100 K. After mass selection by the quadrupole mass filter, $Co_nCOH_2^+$

was allowed to collide with an Ar atom in the reaction cell filled with an Ar gas (99.9999%) at 298 K. The collision energy was adjusted in the range between 1 and 5 eV in the center-of-mass frame. The cations produced by the CID process were identified by the second quadrupole mass analyzer.

2.3. Computational method. DFT calculations were performed by the Gaussian 16 package[19] employing the BPW91 functional[20,21] to search for optimized geometric and electronic structures of Co_n^+ (n = 5, 8, and 9) and their CO and/or H_2 adducts. The LanL2DZ basis set was used for Co with corresponding effective core potential,[22] while the aug-cc-pVTZ basis set was used for C, O, and H.[23,24] The functional and the basis sets were chosen by referring to earlier reports.[25–27] All the possible initial geometries were examined for Co_n^+ including previously reported structures.[27,28] As for CO and/or H_2 adducts, all the possible adsorption sites of CO and H_2 were examined for the optimized Co_n^+ as well as its possible spin multiplicities.

3. RESULTS AND DISCUSSION

3.1. Reaction of $Co_n(CO)_m^+$ with H_2. Figure 1 shows mass spectra of product ions upon reaction of Co_n^+ and $Co_n(CO)^+$ with H_2; panels a–c for Co_n^+, d–f for $Co_n(CO)^+$, and g–i for $Co_n(CO)_2^+$ display n = 8, 9, and 10, respectively. The abscissa shows a mass shift, ΔM, from the reactant. Regarding Co_n^+, a small peak at ΔM = +2 u is assignable to $Co_{10}H_2^+$ for n = 10, whereas no reaction product is discernible for n = 8 and 9. As for $Co_n(CO)^+$, on the other hand, such H_2 adduct is observed for n = 8 and 9 as well as for n = 10. These results suggest that preadsorption of CO on Co_n^+ promotes the reaction with H_2 for any size from n = 8 to 10. The mass spectra of $Co_n(CO)_2^+$ show that formation of H_2 adduct is suppressed with respect to the case of $Co_n(CO)^+$ for each size.

Reactivity measurement toward H_2 was performed for Co_n^+ and $Co_n(CO)_m^+$ (m = 1 and 2) in the range of n = 3–11 to evaluate reaction-rate coefficients, $k_{n,m}$. Pseudo-first-order reaction kinetics is assumed since the concentration of H_2 was kept constant during the reaction. It is derived from the yield of reaction products as follows:

$$k_{n,m} = -[\ln\{I_r/(I_r + \Sigma I_p)\}]/(n_{H2}t), \qquad (2)$$

where n_{H2} is the number density of H_2 in the reaction cell, t the time for the clusters to pass through the reaction cell, I_r and I_p are intensities of the reactant and the product ions, respectively. The time, t, is calculated for each size by converting the translational energy of 7 eV in the laboratory frame to the velocity of the cluster. The rate coefficients thus obtained are shown in Fig. 2 as a function of cluster size, n. The reactivity of CO-free cobalt cluster cations, m = 0, becomes significant only at $n \geq 10$; $k_{n,0}$ is below the detection limit for $n \leq 9$. Note that this result is consistent with the previous report,[7] except that weak signals of H_2 adsorption were observed for n = 3, 4, and 5 as well probably due to a low-temperature buffer He gas present in their reaction cell. On the other hand, the rate coefficients of m = 1 series are clearly higher than those of m = 0 for n = 5 and 8–10; preadsorption of a CO molecule enhances the reactivity in these sizes. At n = 11, in contrast, the rate coefficient of m = 1 is lower than m = 0; CO preadsorption reduces the reactivity. Results of m = 2 show no further enhancement at any size, indicating that H_2 adsorption is rather suppressed by the second CO molecule.

3.2. Change in reactivity by CO preadsorption. The rate coefficient of H_2 adsorption on Co_n^+ is altered by preadsorption of CO as manifested in Figs. 1 and 2. The earlier study explained reactivity of H_2 adsorption by the frontier orbital model,[7] pointing out importance of interaction between the LUMO of H_2 and the HOMO of metal clusters; the H–H bond is activated when the H_2 molecule acts as an acceptor of electrons donated by the metal cluster.[29] Here we apply this

model to our present results. The electronic levels in Co_n^+ are expected to be modified by preadsorption of CO because it is known for a transition-metal surface that a CO molecule is chemisorbed through concerted electron transfer from the HOMO of CO to the metal and back-donation from the metal to the LUMO of CO.[30,31] The change in the energy levels of clusters should, therefore, affect their reactivity toward H_2 by modulating the magnitude of interaction between the LUMO of H_2 and molecular orbitals (MOs) of the cluster.

In this context, we performed DFT calculations to investigate MO energies of Co_n^+ and $Co_n(CO)_m^+$ for n = 5 and 8–10, where reactivity shows significant changes by CO preadsorption. Optimized structures of Co_n^+, $Co_n(CO)^+$, $Co_n(CO)_2^+$, and their H_2 adducts are shown in Fig. S1 of the Supporting Information along with their spin multiplicities, $2S$+1. The spin multiplicities, 11, 18, 19, and 20 for Co_5^+, Co_8^+, Co_9^+, and Co_{10}^+, respectively, are consistent with previous studies.[27,32,33] CO and H_2 are adsorbed on Co_n^+ in end-on and side-on configurations, respectively. Note that side-on configuration for CO was not found even as a metastable isomer; end-on configurations for H_2 were higher by more than 4 eV than the side-on configuration. Figure S1 also shows contours of MOs for each cluster; for H_2 adducts, the highest occupied MO among those involved in bonding with H_2 is displayed, whereas MO with a similar symmetry is depicted for the corresponding H_2-free clusters. The relative energies of these MOs, which were thus found to contribute to H_2 binding, are illustrated in Fig. 3 with respect to the energy of LUMO of H_2. For CO-free Co_n^+, the MO energy increases in the order of $Co_5^+ < Co_8^+ < Co_9^+$. The energy of the MO is modified by CO preadsorption. For example, the MO of Co_8^+ is raised by adsorption of CO, whereas the second CO lowers the level. The energy order is thus $Co_8^+ < Co_8(CO)_2^+ < Co_8(CO)^+$, which is the same trend as their reactivity shown in Fig. 2. This result suggests that higher reactivity is expected if the MO of the cluster is closer to the LUMO of H_2 in energy. This

discussion holds for n = 5, 9, and 10 as well, where the order of the MO energies of CO adducts is correlated with their reactivity. We thus found that the reactivity is governed by the MO energy of the cluster, which can be tuned by preadsorption of CO. On the other hand, we also examined relative energies of the LUMO of the clusters against the HOMO of H_2, because it has been reported that electron donation from H_2 to a transition metal occurs in concert with that from the metal to H_2.[34,35] However, no clear correlation with reactivity was found in this case. These findings support that the present reactivity toward H_2 is dominated by the energy difference between the HOMO of the cluster and the LUMO of H_2, as suggested by previous studies on CO-free cobalt cluster cations.[7,29]

3.3. Reaction between coadsorbed CO and H_2. CID experiments were performed on $Co_nCOH_2^+$ (n = 8–10) to identify the product formed on Co_n^+. A mass spectrum of ions recorded for $Co_8COH_2^+$ is shown in Fig. 4 upon collision with Ar at 2.4 eV in the center-of-mass frame. Peaks observed at ΔM = −2 and −28 u are assigned to ions produced via dissociation of H_2 and CO, respectively. The peak at ΔM = −30 u might have two origins: one is dissociation of a molecule formed by reaction between CO and H_2, possibly formaldehyde H_2CO, and the other is sequential dissociation of CO and H_2 molecules. Major processes are represented by ΔM = −2 and −30 u, while ΔM = −28 u shows a very minor dissociation channel.

Figure 5 shows partial cross sections of each CID channel of $Co_8COH_2^+$. The cross section was estimated by the following equation:

$$\sigma_{\Delta M} = [-\ln\{I_R/(I_R + \Sigma I_P)\}/(n_{Ar}l)] \times (I_{\Delta M} / \Sigma I_P), \quad (3)$$

where n_{Ar} is the number density of Ar in the reaction cell, l the length of the reaction cell, I_R, I_P, and $I_{\Delta M}$ are intensities of the reactant ion, $Co_8COH_2^+$, the product ions, and the ion at ΔM among the products, respectively. For ΔM = −30 u (Fig. 5a), the partial dissociation cross section exhibits

an increasing trend with the collision energy. On the other hand, the cross section of CO dissociation ($\Delta M = -28$ u) is very small over the range of the present collision energies. This is in contrast to the result for H_2-free Co_8CO^+, where it is much larger than of $Co_8COH_2^+$ as superimposed in Fig. 5b. This result implies that CO adsorption is not just physisorption any more in the presence of H_2 coadsorbed. It is thus highly probable that some of the CO and H_2 molecules are bound together on Co_n^+, which is readily released by collision with Ar. Note that a major part of H_2 remains molecular on Co_8^+ because H_2 release shows a large cross section as manifested in Fig. 5c. The results suggest, therefore, that a major part of CO is chemisorbed or dissociatively adsorbed on Co_8^+, while some of the CO react with H_2 to form H_2CO.

The results of CID experiment for $Co_9COH_2^+$ and $Co_{10}COH_2^+$ are shown in Figs. S2 and S3 of the Supporting Information, respectively. The cross sections of CO dissociation ($\Delta M = -28$ u) from $Co_9COH_2^+$ and $Co_{10}COH_2^+$ are much smaller than that from Co_8CO^+ as in the case of $Co_8COH_2^+$. It is speculated for Co_9^+ and Co_{10}^+ as well as for Co_8^+ that CO and H_2 might be bound together, even though those partial cross sections of $\Delta M = -30$ u are smaller than $Co_8COH_2^+$.

4. CONCLUSIONS

We investigated gas-phase reactions of free cobalt clusters and their CO complexes, Co_n^+ and $Co_n(CO)_m^+$ (n = 3–11; m = 1, 2), with H_2 to examine formation of an organic molecule, possibly formaldehyde, through catalytic reaction. The rate coefficient of H_2 adsorption was found to be altered by CO pre-adsorption on Co_n^+. DFT calculation suggested that the reactivity is governed by the MO energy of the clusters that interacts with the LUMO of H_2; the MO energy is tuned by preadsorption of CO molecules. CID experiment performed on $Co_nCOH_2^+$ (n = 8–10) implied that the coadsobed CO and H_2 are bound together, at least partially, on Co_n^+.

ASSOCIATED CONTENT

Supporting Information

The Supporting Information is available free of charge on the ACS Publications website at DOI: xxx. Optimized structures of Co_n^+, $Co_n(CO)^+$, $Co_n(CO)_2^+$, and their H_2 adducts for n = 5, 8, and 9, along with isosurface of the highest molecular orbital interacting with the H_2 molecule. Partial dissociation cross sections of each ion produced from $Co_9COH_2^+$ and $Co_{10}COH_2$ as a function of collision energy. A complete list of authors of ref. 19.

AUTHOR INFORMATION

Corresponding Authors

* (M.A.) E-mail: arakawa@chem.kyushu-univ.jp

* (A.T.) E-mail: terasaki@chem.kyushu-univ.jp

Notes

The authors declare no competing financial interest.

ACKNOWLEGEMENTS

This work was supported by Grants-in-Aid for Scientific Research (A) (JP18H03901) and for Scientific Research (C) (JP19K05185) from the Japan Society for Promotion of Science (JSPS),

and for Scientific Research on Innovative Areas (JP16H00938 and JP17H06456) from the Ministry of Education, Culture, Sports, Science and Technology (MEXT). The computational work was carried out by the computer facilities at Research Institute for Information Technology, Kyushu University.

REFERENCES

(1) Lang, S. M.; Bernhardt, T. M. Gas Phase Metal Cluster Model Systems for Heterogeneous Catalysis. *Phys. Chem. Chem. Phys.* **2012**, *14*, 9255−9269.

(2) Nuth, J. A.; Johnson, N. M.; Manning, S. A Self-Perpetuating Catalyst for the Production of Complex Organic Molecules in Protostellar Nebulae. *Astrophys. J.* **2008**, *673*, L225−L228.

(3) Arakawa, M.; Yamane, R.; Terasaki, A. Reaction Sites of CO on Size-Selected Silicon Oxide Cluster Anions: A Model Study of Chemistry in the Interstellar Environment. *J. Phys. Chem. A* **2016**, *120*, 139−144.

(4) Arakawa, M.; Omoda, T.; Terasaki, A. Adsorption and Subsequent Reaction of a Water Molecule on Silicate and Silica Cluster Anions. *J. Phys. Chem. C* **2017**, *121*, 10790−10795.

(5) Lee, S.; Lee, B.; Seifert, S.; Winans, R. E.; Vajda, S. Fischer−Tropsch Synthesis at a Low Pressure on Subnanometer Cobalt Oxide Clusters: The Effect of Cluster Size and Support on Activity and Selectivity. *J. Phys. Chem. C* **2015**, *119*, 11210–11216.

(6) Morse, M. D.; Geusic, M. E.; Heath, J. R.; Smalley, R. E. Surface Reactions of Metal Clusters. II. Reactivity Surveys with D_2, N_2, and CO. *J. Chem. Phys.* **1985**, *83*, 2293–2304.

(7) Nakajima, A.; Kishi, T.; Sone, Y.; Nonose, S.; Kaya, K. Reactivity of Positively Charged Cobalt Cluster Ions with CH_4, N_2, H_2, C_2H_4, and C_2H_2. *Z. Phys. D: At., Mol. Clusters* **1991**, *19*, 385–387.

(8) Liu, F.; Armentrout, P. B. Guided Ion-Beam Studies of the Kinetic-Energy-Dependent Reactions of Co_n^+ (n = 2–16) with D_2: Cobalt Cluster-Deuteride Bond Energies. *J. Chem. Phys.* **2005**, *122*, 194320.

(9) Guo, B. C.; Kerns, K. P.; Castleman, A. W., Jr. Chemistry and Kinetics of Size-Selected Cobalt Cluster Cations at Thermal Energies. I. Reactions with CO. *J. Chem. Phys.* **1992**, *96*, 8177–8186.

(10) Fielicke, A.; von Helden, G.; Meijer, G.; Pedersen, D. B.; Simard, B.; Rayner, D. M. Size and Charge Effects on the Binding of CO to Late Transition Metal Clusters. *J. Chem. Phys.* **2006**, *124*, 194305.

(11) Swart, I.; Fielicke, A.; Rayner, D. M.; Meijer, G.; Weckhuysen, B. M.; de Groot, F. M. F. Controlling the Bonding of CO on Cobalt Clusters by Coadsorption of H_2. *Angew. Chem. Int. Ed.* **2007**, *46*, 5317–5320.

(12) Hanmura, T.; Ichihashi, M.; Watanabe, Y.; Isomura, N.; Kondow, T. Reactions of Nitrogen Monoxide on Cobalt Cluster Ions: Reaction Enhancement by Introduction of Hydrogen. *J. Phys. Chem. A* **2007**, *111*, 422–428.

(13) Ito, T.; Naresh, G. P.; Arakawa, M.; Terasaki, A. Water-Induced Adsorption of Carbon Monoxide and Oxygen on the Gold Dimer Cation. *J. Phys. Chem. A* **2014**, *118*, 8293–8297.

(14) Terasaki, A.; Majima, T.; Kondow, T. Photon-trap Spectroscopy of Mass-Selected Ions in an Ion Trap: Optical Absorption and Magneto-Optical Effects. *J. Chem. Phys.* **2007**, *127*, 23110.

(15) Arakawa, M.; Ando, K.; Fujimoto, S.; Mishra, S.; Naresh Patwari, G.; Terasaki, A. The Role of Electronegativity on the Extent of Nitridation of Group 5 Metals as Revealed by Reactions of Tantalum Cluster Cations with Ammonia Molecules. *Phys. Chem. Chem. Phys.* **2018**, *20*, 13974–13982.

(16) Ito, T.; Egashira, K.; Tsukiyama, K.; Terasaki, A. Oxidation Processes of Chromium Dimer and Trimer Cations in an Ion Trap. *Chem. Phys. Lett.* **2012**, *538*, 19−23.

(17) Griffin, J. B.; Armentrout, P. B. Guided Ion Beam Studies of the Reactions of Cr_n^+ (n = 2–18) with O_2: Chromium Cluster Oxide and Dioxide Bond Energies. *J. Chem. Phys.* **1998**, 108, 8062–8074.

(18) Gioumousis, G.; Stevenson, D. P. Reactions of Gaseous Molecule Ions with Gaseous Molecules. V. Theory. *J. Chem. Phys.* **1958**, *29*, 294−299.

(19) Frisch, M. J.; Trucks, G. W.; Schlegel, H. B.; Scuseria, G. E.; Robb, M. A.; Cheeseman, J. R.; Scalmani, G.; Barone, V.; Petersson, G. A.; Nakatsuji, H.; et al. *Gaussian 16*, revision A.03; Gaussian, Inc.: Wallingford, CT, 2016.

(20) Becke, A. D. Density-Functional Exchange-Energy Approximation with Correct Asymptotic Behavior. *Phys. Rev. A* **1988**, *38*, 3098−3100.

(21) Perdew, J. P.; Wang, Y. Accurate and Simple Analytic Representation of the Electron-Gas Correlation Energy. *Phys. Rev. B* **1992**, *45*, 13244−13249.

(22) Hay, P. J.; Wadt, W. R. Ab Initio Effective Core Potentials for Molecular Calculations. Potentials for K to Au Including the Outermost Core Orbitals. *J. Chem. Phys.* **1985**, 82, 299−310.

(23) Dunning, T. H., Jr. Gaussian Basis Sets for Use in Correlated Molecular Calculations. I. The Atoms Boron Through Neon and Hydrogen. *J. Chem. Phys.* **1989**, *90*, 1007−1023.

(24) Kendall, R. A.; Dunning, T. H., Jr.; Harrison, R. J. Electron Affinities of the First-Row Atoms Revisited. Systematic Basis Sets and Wave Functions. *J. Chem. Phys.* **1992**, *96*, 6796−6806.

(25) Gutsev, G. L.; Weatherford, C. W.; Belay, K. G.; Ramachandran, B. R.; Jena, P. An All-Electron Density Functional Theory Study of the Structure and Properties of the Neutral and Singly Charged M_{12} and M_{13} clusters: M = Sc–Zn. *J. Chem. Phys.* **2013**, *138*, 164303.

(26) de Souza Monteiro, R.; Paes, L. W. C.; de M. Carneiro, J. W.; Aranda, D. A. G. Modeling the Adsorption of CO on Small Pt, Fe and Co Clusters for the Fischer–Tropsch Synthesis. *J. Clust. Sci.* **2008**, *61*, 601−614.

(27) Hirabayashi, S.; Ichihashi, M. Ammonia Dehydrogenation on Cobalt Cluster Cations Doped with Niobium. *Top. Catal.* **2018**, *61*, 35−41.

(28) Datta, S.; Kabir, M.; Ganguly, S.; Sanyal, B.; Saha-Dasgupta, T.; Mookerjee, A. Structure, Bonding, and Magnetism of Cobalt Clusters from First-Principles Calculations. *Phys. Rev. B* **2007**, *76*, 014429.

(29) Fayet, P.; Kaldor, A.; Cox, D. M. Palladium Clusters: H_2, D_2, N_2, CH_4, CD_4, C_2H_4, and C_2H_6 Reactivity and D_2 Saturation Studies. *J. Chem. Phys.* **1990**, *92*, 254–261.

(30) Blyholder, G. Molecular Orbital View of Chemisorbed Carbon Monoxide. *J. Phys. Chem.* **1964**, *68*, 2772–2777.

(31) Doyen, G.; Ertl, G. Theory of Carbon Monoxide Chemisorption on Transition Metals. *Srf. Sci.* **1974**, *43*, 197–229.

(32) Gehrke, R.; Gruene, P.; Fielicke, A.; Meijer, G.; Reuter, K. Nature of Ar Bonding to Small Clusters and its Effect on the Structure Determination by Far-Infrared Absorption Spectroscopy. *J. Chem. Phys.* **2009**, *130*, 034306.

(33) Kiawi,D. M.; Bakker, J. M.; Oomens, J.; Buma, W. J.; Jamshidi, Z.; Visscher, L.; Waters, L. B. F. M. Water Adsorption on Free Cobalt Cluster Cations. *J. Phys. Chem. A* **2015**, *119*, 10828–10837.

(34) Kubas, G. J. Molecular Hydrogen Complexes: Coordination of a σBond to Transition Metals. *Acc. Chem. Res.* **1988**, *21*, 128–134.

(35) Kubas, G. J. Metal–Dihydrogen and σ-Bond Coordination: the Consummate Extension of the Dewar–Chatt–Duncanson Model for Metal–Olefin π Bonding. *J. Organomet. Chem.* **2001**, *635*, 37–68.

FIGURES

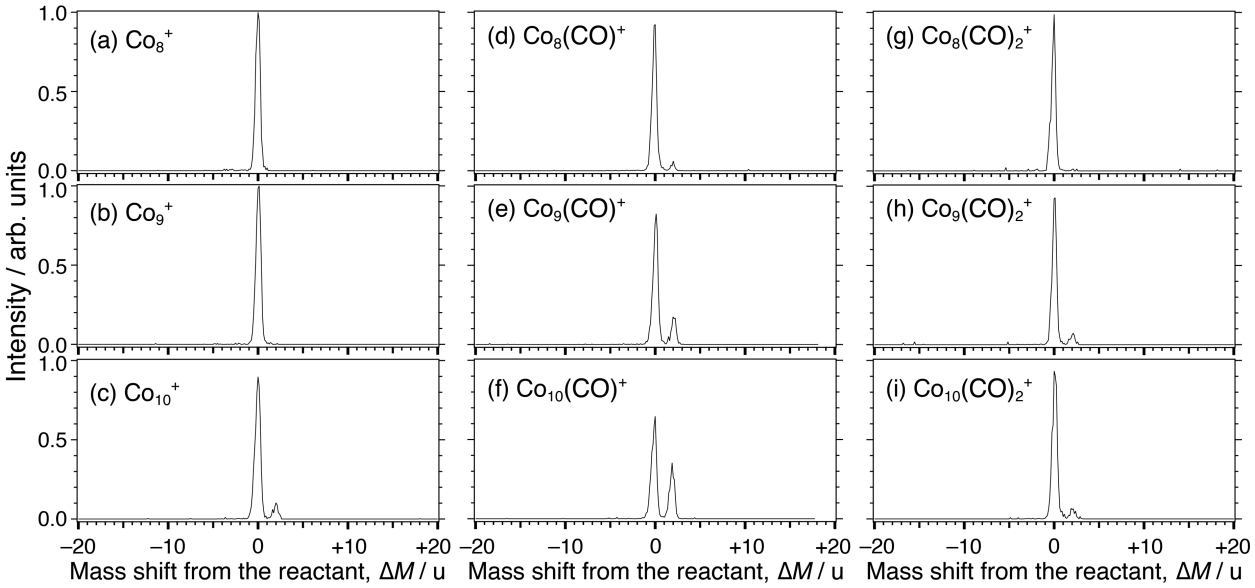

Figure 1. Mass spectra of ions produced in the reaction of (a) Co_8^+, (b) Co_9^+, (c) Co_{10}^+, (d) $Co_8(CO)^+$, (e) $Co_9(CO)^+$, (f) $Co_{10}(CO)^+$, (g) $Co_8(CO)_2^+$, (h) $Co_9(CO)_2^+$, and (i) $Co_{10}(CO)_2^+$ with a H_2 molecule. The partial pressure of H_2, P_{H2}, was 4×10^{-1} Pa. The intensity was normalized so that the summation of the peak intensity of all the reactant and product ions is to be unity.

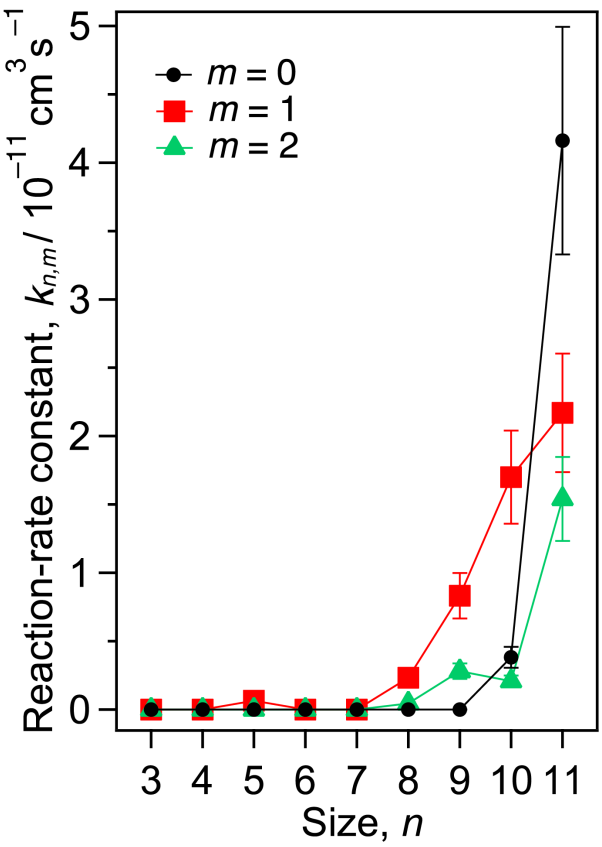

Figure 2. Size-dependent rate coefficient of $Co_n(CO)_m^+$ for reaction with a H_2 molecule. Error bars indicate a systematic error of 20% due to the uncertainty in the partial pressure of H_2 in the reaction cell.

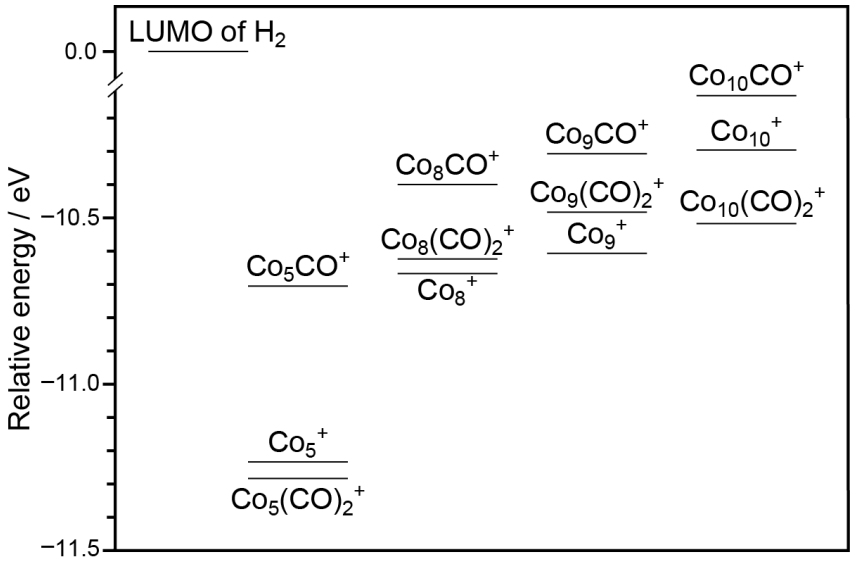

Figure 3. Relative energies of MOs of Co_n^+, $Co_n(CO)^+$, and $Co_n(CO)_2^+$ that interact with H_2 for n = 5, 8, 9, and 10. The energies are with respect to the LUMO of H_2.

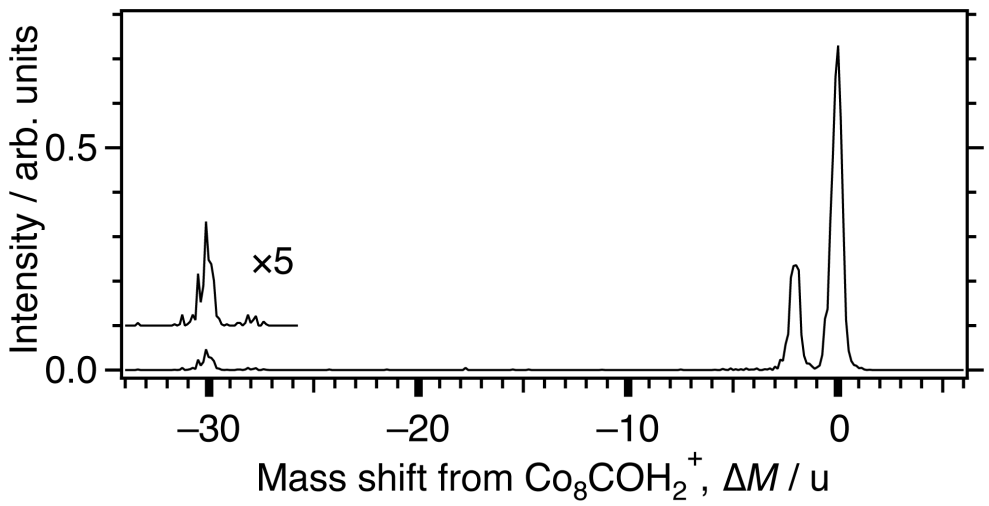

Figure 4. A CID mass spectrum recorded for $Co_8COH_2^+$ upon collision with Ar at 2.4 eV in the center-of-mass frame. ΔM is a mass shift from $Co_8COH_2^+$. A magnified spectrum in the vicinity of $\Delta M = -30$ u is superimposed.

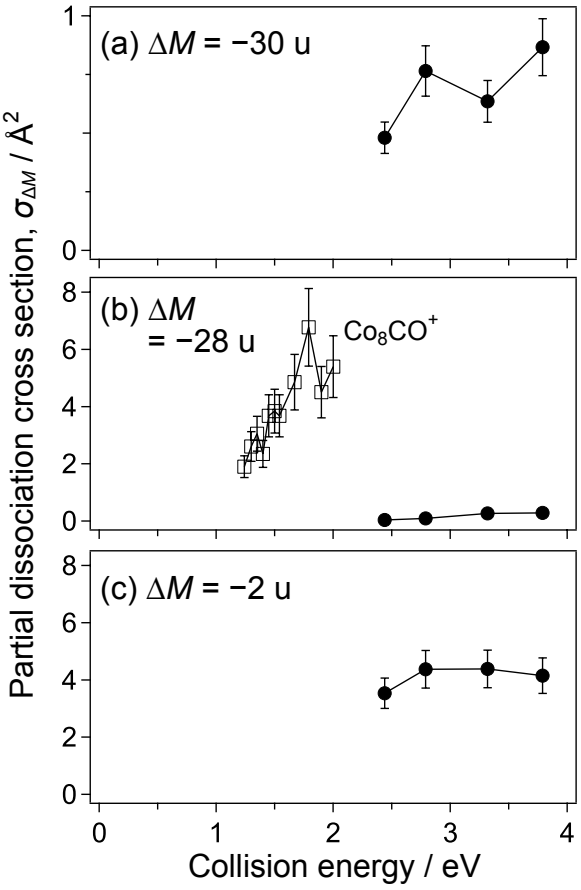

Figure 5. Partial dissociation cross sections as a function of collision energy mesured for $Co_8COH_2^+$ to the pathways with loss of (a) 30 u, (b) 28 u (CO), and (c) 2 u (H_2). Dissociation cross sections of CO release from Co_8CO^+ are superimposed in (b). Error bars indicate statistical uncertainies.

TOC Graphic

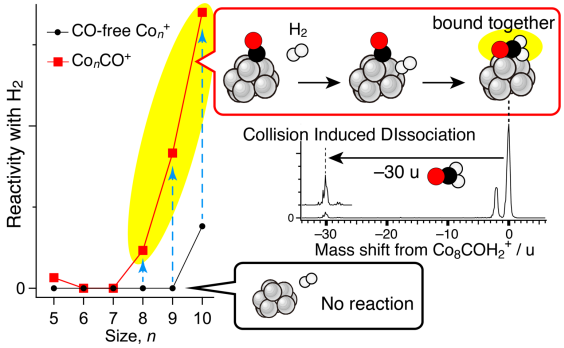
CO-free Co$_n^+$
Co$_n$CO$^+$
Reactivity with H$_2$
0
5 6 7 8 9 10
Size, n
H$_2$
bound together
Collision Induced DIssociation
–30 u
0
–30 –20 –10 0
Mass shift from Co$_8$COH$_2^+$ / u
No reaction